Influcence of interface diffusion on pearlite growth: A phase-field study

A Thesis

Submitted for the Degree of

Master of Engineering

in the **Faculty of Engineering**

by

Ajaya Pratap Jena

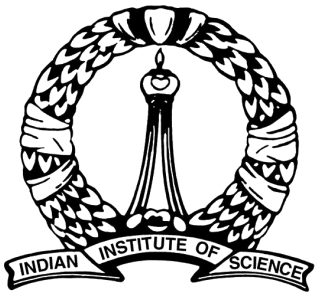

Department of Materials Engineering
Indian Institute of Science
Bangalore – 560 012 (INDIA)

JUNE 2017

DEDICATED TO

my Parents and Teachers

Signature of the Author: .....

Ajaya pratap Jena

Dept. of Materials Engineering

Indian Institute of Science, Bangalore

Signature of the Thesis Supervisor: .....

Dr. Abhik Choudhury

Assistant Professor

Dept. of Materials Engineering

Indian Institute of Science, Bangalore

Acknowledgements

I express my sincere gratitude towards my research advisor Prof. Abhik Choudhury for the guidance and support he extended to me throughout my stay in IISc. He has played the key role in enriching my knowledge in the field of computational material science through his excellent lectures during his course and also our regular discussions during the project. He has always been kind and patient with me whenever I asked him doubts, however silly they might be. It was his friendly behavior, enthusiasm for our work, attitude towards the problems, and his occasional rebukes, that kept me motivated throughout the course and helped me complete my research work successfully. I am highly thankful as well as grateful to him for the same.

I would like to thank prof T A Abhinandanan, chairman, Department of Materials Engineering, for providing all the facilities of the department. He has always been cheerful and friendly towards us. His insightful questions and useful discussions gave me new directions in my work. I would also like to thank Prof S. Kartikeyan, Prof Praveen Kumar, Prof Satyam Suwas, Prof Aloke Paul and Prof Chandan Srivastava for their wonderful lectures during the course work.

This acknowledgement would remain incomplete without the group of people I dedicate the next few lines, who also form an integral part of my 2^{nd} year of Masters. I take this opportunity to thank all my lab mates, without whose efforts I could not have possibly completed my work. I start by thanking Arka Lahiri, the godfather of our Lab, who helped me whenever

I used to get stuck, following which I thank Balachandra Bhadak, Pramod Sharma, Supriyo Chakraborty, A Shanmukha Kiran, Fiyanshu Kaka and Pradeep Kudagi. I am pleased to work beside these extremely talented and cool set of people. I hope they excel in their future as good as they are excelling now.

Next, I would like to acknowledge my fellow batchmates few of whom formed the inner circle of my personal life here at IISc. I begin by thanking Sneha and Anuj for being the closest friends, with whom I have spent the majority of my free time. I will miss the intellectual discussions, the mandatory weekend dinner-outs, the meaningless conversations and also the ocassional quarells I had with you guys. I also thank Gyan and Puneet for teaching me TT. I will remember the exciting trips I went with Ankush and Subham in the first year. I would also like to acknowledge Abhijeet and Ankita for helping me during the placement season. I will miss my bengali friends Soudip, Sarabjeet and Soham who always wished good for me and also unintentionally taught me bengali.

Abstract

Pearlite has been a subject of theoretical and experimental studies, since the inception of steel as a structural material. The classical Zener-Hillert theory[12, 5] has developed a preliminary understanding of the growth mechanisms occurring during the transformation. Volume diffusion was considered as the limiting factor for growth, however the results are roughly an order of magnitude off from what is observed in experiment. Hence subsequent theories by Sundquist[11] and Hillert[6] came into picture, considering interface diffusion as the dominant mechanism, which reduced the gap between theoretical and experimental results to some extent. Recently numerical studies have been attempted by Nakajima et al. and Steinbach I[8] to understand the problem in greater detail. Despite significant efforts in this domain, a computational model accounting for both volume and interface diffusion does not exist. In this thesis we study the influence of interface diffusion on lamellar growth of pearlite during its transformation with the help of phase-field simulations.

We start by extending the classical Jackson Hunt analysis to accommodate contribution from both the mechanisms i.e. bulk diffusion and interface diffusion. The analysis gives a relation between velocity, inter-lamellar spacing and under-cooling. For this study we impose isothermal condition for which under-cooling remains constant and the velocity(v) vs Inter-lamellar spacing(λ) curve looks like an inverted U. The system chooses the maximally growing velocity v_{max} and the λ corresponding to it. The analytical calculation performed in chapter 3 predicts

that at a constant under-cooling, addition of interface diffusion increases the growth velocity however it does not effect inter-lamellar spacing chosen by the system. This analytical prediction is in line with Zener's theory. This behavior is reproduced using a quantitative multi-phase field model.

Our model includes the thermodynamics of Fe-C binary system for the numerical study of the above phenomena. The thermodynamics of the system, particularly the variation of free energy with composition, is obtained from thermo-calc database. Thereafter, a data-fitting procedure is described to approximate the variation of grand-potentials[3] of the respective phases as a function of chemical potential. This is done by fitting parabolas to the energy curves of different phases at their respective equilibrium compositions. A novel quantitative phase-field model is used to simulate pearlite growth by adding a interface mobility term to the mobility parameter in the evolution equation. The model is initially run with only bulk diffusion in order to have a close match with the analytical curve. This is an important step in the work as it provides us with a model which can correctly capture the thermodynamics of pearlite transformation and can reproduce the behavior predicted by analytical curve within 20% tolerance.

Subsequently, simulations were performed with different values of interface diffusion to understand its effect on the growth kinetics. It is observed that with increasing values of interface diffusion the velocity vs lambda curve shifts upwards without any change in the spacing. This supports our hypothesis predicted by analytical calculation. Further, we study the effect of asymmetric mobilities of ferrite and cementite phase. Finally we plan to extend the model to ternary systems to understand the effect of addition of third component on pearlite growth kinetics, however this work is not a part of this thesis.

Contents

List of Figures

Chapter 1

Introduction

Pearlite is an extremely useful phase of steel that has varied applications which typically includes rails, ropes for bridges and elevators, steel cord for tire reinforcement etc. It is an inter penetrating bi-crystal of ferrite(α) and cementite (β) that forms as a result of eutectoid transformation from austenite(γ). It is essentially a lamellar structure where the inter-lamellar spacing plays an important role in tailoring the mechanical properties. Since the discovery of pearlite numerous work has been done, the majority of which includes that of Zener[12] and Hillert[5] who established the relation between lamellar spacing, velocity and under cooling during pearlite transformation. However the Zener-Hillert model shows large deviations from the experimentally measured lamellar growth velocities. Their model assumes diffusion in the austenite phase only, which might not hold good for eutectoid reaction since it is a solid state transformation where the diffusivity in the product and parent phases are comparable. Broadly two prime mechanisms of pearlite transformation has been reported in literature, i.e. volume diffusion and interface diffusion. Despite large amounts of effort a clear understanding of the mechanism of pearlite transformation has not been clearly established.

1.1 Motivation

Pearlite transformation basically falls under the realm of moving boundary problems. It is essentially a co-operative growth of two solid phases into another solid phase. Recently, phase-field models have been used to gain insights into pearlite growth. Nakajima et.al.[8] used the multi phase-field method to simulate the co-operative pearlite growth by accounting for diffusion in the ferrite as well as the austenite phase. They predict a successive process of diffusion in ferrite and growth of cementite from the ferrite, resulting in an increase of the kinetics of pearlitic transformation by a factor of four as compared to growth from austenite exclusively. Steinbach and plapp[10] claim an overlap of phase-field results with Hillerts model in absence of diffusion in ferrite. Further, they couple a stress-driven diffusion field to the phase field and study the effect of transformation strains. However, Pandit and Bhadeshia[9] argue that pearlite forms by re-constructive transformation, in which case, transformation strains should not be significant. They also emphasize the need to consider both the mechanisms, bulk as well as interface diffusion simultaneously for an overlap with experimental findings. The present work derives motivation from the fact that a numerical model considering both volume and interface diffusion does not exist. It is aimed at developing an understanding of pearlite growth mechanisms using phase field simulations by considering both bulk and interface diffusivity in the model. The classical Jackson Hunt analysis for eutectic transformation is extended to incorporate both the mechanisms. A close match of the analytical prediction and numerical results from the phase-field model is targeted.

1.2 Phase-field model

The Phase field model is a diffuse interface model where the interface is assumed to have a definite width in contrast to sharp interface models. Sharp interface models have a steep jump

of parameters across the interface which is associated with singularities. Hence these models are computationally costly both in space and time. This problem is eliminated in phase-field method where the position of the interface is taken care by an order parameter(ϕ) which evolves with time indicating the movement of the interface. The value of the order parameter for a certain phase represents the presence or absence of the phase. The free energy of the system is defined in terms of the phase field variables and the order parameter is restricted to evolve in a direction which tends to lower its free energy. This results in a micro structure which forms with morphological changes in different phases as guided by the imposed conditions of the phase filed variables e.g. temperature, under-cooling, velocity etc. Broadly two types of phase field equations are used, the Cahn-Hillard equation and the Allen-Cahn equation. The Cahn-Hilliard equation uses a conserved order parameter to define the phase field whereas the Allen-Cahn equation uses a non-conserved order parameter. Both the equations have their respective usage in micro structure evolution. Cahn-Hillard equation is used where masses of different phases are conserved e.g. during ostwald ripening the precipitate phase coarsen but the mass is conserved. Allen-Cahn equation is used where masses are non-conserved as an example in solidification, solid grows and liquid decreases. This justifies the use of phase-field model for the present problem of solid state phase transformation.

Chapter 2

Literature review

Before we begin developing theory for investigating the influence of interface diffusion it is essential to understand the classical theories established by pioneers in this field. This chapter gives a brief overview of the important theories that carved the present understanding about the mechanisms of pearlite growth. There are two principal mechanisms cited in the literature to explain the kinetics of pearlite growth, one involves the volume diffusion of carbon ahead of the transformation front, while the other relies on interface diffusion as the rate-controlling step. These mechanisms give us a relation between growth velocity and lamellar spacing, however the system chooses a particular v and λ based on certain criterion. This criteria fixes the velocity and spacing for the system. Broadly two criteria are present in literature which has been explained in the second part of this chapter with fair bit of detail.

2.1 Mechanisms of Pearlite growth

2.1.1 Volume diffusion

According to Zener-Hillert theory, during the growth of pearlite, carbon is transported from the edges of the ferrite lamella to neighboring cementite lamella[12][5]. The diffusion is assumed to

occur only via parent austenite phase. The ferrite-austenite and cementite-austenite interfaces are also assumed to be flat where the concentration of austenite in equilibrium with ferrite and cementite is given by $c_e^{\gamma\alpha}$ and $c_e^{\gamma\theta}$ respectively. Zener suggested that the real concentration can be approximated to be $\left(1 - \frac{S_c}{S}\right)\left(c_e^{\gamma\alpha} - c_e^{\gamma\theta}\right)$ because of the energy penalty due to formation of interfaces. Out of the total free energy available for pearlite transformation a part of it goes for the creation of the interfaces between ferrite and cementite which is given by

$$\Delta G_m^{surface} = \frac{2\sigma^{\alpha\theta} V_m}{S} \tag{2.1}$$

where $\sigma^{\alpha\theta}$ is the interface energy per unit area and V_m is the molar volume of austenite. As the inter-lamellar spacing decreases, more and more of the available free energy is converted into interface energy until a critical spacing S_c, is reached where all the available free energy is consumed in the creation of interfaces. Thus

$$\Delta G_m^{surface} = \frac{2\sigma^{\alpha\theta} V_m}{S_c} \tag{2.2}$$

The free energy is thus reduced by a factor of

$$\frac{\Delta G_m^{total} - \Delta G_m^{surface}}{\Delta G_m^{total}} = \left(1 - \frac{S_c}{S}\right) \tag{2.3}$$

The diffusion of carbon from the tip of ferrite up to a cementite lamella can be represented as

$$J = \frac{-A_\alpha}{V_m} D_C^\gamma \frac{\partial c}{\partial x} = \frac{2 D_c^\gamma S^\alpha b}{V_m} \frac{\left(c_e^{\gamma\alpha} - c_e^{\gamma\theta}\right)}{S^\alpha} \tag{2.4}$$

where J is the carbon flux, V_m is the molar volume and is considered same for all the phases involved, and A_α is the cross sectional area of the the interface, which is equal to $S^\alpha b$, where b is an arbitrary distance perpendicular to the growth direction. The stefan condition at the

interface writes as

$$J = \frac{vbS^{\alpha}}{V_m}(\overline{c_e} - c_e^{\alpha\gamma}) = \frac{vbS^{\theta}}{V_m}(c_e^{\alpha\gamma} - \overline{c_e}) = \frac{vbS^{\alpha}S^{\theta}}{SV_m}(c_e^{\theta\gamma} - c_e^{\alpha\gamma}) \tag{2.5}$$

where S^{α} and S^{θ} represent the thickness of ferrite and cementite lamella. A modification of the above equation gives the relation between v and S as

$$v = \frac{2D_c^{\gamma}S}{S^{\alpha}S^{\theta}}\left(\frac{c_e^{\gamma\alpha} - c_e^{\gamma\theta}}{c_e^{\theta\gamma} - c_e^{\alpha\gamma}}\right) \tag{2.6}$$

2.1.2 Interface diffusion

The principal reason behind the attempt to introduce boundary diffusion is the inability of the volume diffusion to account for experimentally observed growth rates in Fe-C alloys, rates which are usually higher than expected. This led to development of alternate mechanism for the transport of solute and the interface diffusion theory seemed to be the most plausible explanation. Sundquist[11] assumed the interface diffusion of carbon to be a dominant mechanism driving the edgewise growth of pearlite. The growth rate was calculated using the assumption of local equilibrium and included the effect of capillarity. Using the experimental data for pearlite growth velocity for Fe-C steels, the activation energy for interface diffusion calculated was far too high. Although, it was attributed to the presence of impurity atoms present in the steel, the justification seems to be unrealistic. Hillert modified Zeners volume diffusion theory for the interface diffusion controlled growth[6]. The diffusion flux through the boundary can be written as

$$J = \frac{-A_{\alpha}}{V_m}D_B\frac{\partial c}{\partial x} = \frac{8sD_B\delta S^{\alpha}b}{V_m}\frac{(c_e^{\gamma\alpha} - c_e^{\gamma\theta})}{S^{\alpha}}\left(1 - \frac{S_c}{S}\right) \tag{2.7}$$

where s is the segregation coefficient between the boundary and the austenite phase, δ is the thickness of the boundary layer and is an arbitrary distance perpendicular to the growth

direction. Combining this equation with the mass conservation equation the relation for velocity can be derived as follows

$$v = \frac{8D_B\delta}{S^\alpha S^\theta}\left(\frac{c_e^{\gamma\alpha} - c_e^{\gamma\theta}}{c_e^{\theta\gamma} - c_e^{\alpha\gamma}}\right)\left(1 - \frac{S_c}{S}\right) \tag{2.8}$$

For many alloy systems, when the partitioning of the substitutional element, X, is significant during the growth of pearlite, it is likely that interface diffusion of alloying elements may control the growth of pearlite. The bulk diffusivity of substitutional alloying element is much smaller than that of carbon. As a result, the substitutional elements diffuse through the boundary which provides a faster diffusion path and partition into the product phases[5]. The interface diffusion-controlled growth rate, v_B would be

$$v_B = \frac{12sD_B\delta}{S^\alpha S^\theta}\left(\frac{c_X^{\gamma\alpha} - c_X^{\gamma\theta}}{\overline{c}_X}\right)\left(1 - \frac{S_c}{S}\right) \tag{2.9}$$

where s, the boundary segregation coefficient, is the ratio between alloying element concentration in austenite near the boundary and at the boundary, $c_X^{\gamma\alpha}$ and $c_X^{\gamma\theta}$ are the concentrations of X in austenite which is equilibrium with ferrite and cementite and $\overline{c}_X$ is the bulk concentration of the alloying element in steel.

Cahn and Hagel took a different approach and tried to check the consistency between the measured growth rate, inter-lamellar spacing and the diffusivity. They considered a kinetic parameter β_i, which gave a measure of resistance to segregation. It was suggested that there exists one such parameter for each element and each phase[2]. Cahn and Hagel showed that the apparent diffusivity D_{app} are higher than the D_i (or the experimental diffusivity) by orders of magnitude for non ferrous pearlite however there was reasonable agreement between D_{app} and D_c^γ in plain carbon steels which led to the conclusion that carbon diffusion in austenite controls the pearlite growth in steels.

2.1.3 Mixed diffusion controlled

The first elegant attempt to model a mixed diffusion control growth of pearlite was done by Hashiguchi and Kirkaldy[4] where they assumed a parallel flow of mass through bulk austenite and the pearlite-austenite interface along with capillarity effect and mechanical equilibrium at the interface junctions. The ratio of composition of austenite in contact with cementite and ferrite was kept constant despite the fact that interface energies of $\sigma_{\gamma\alpha}$ and $\sigma_{\gamma\theta}$ were supposed to be different. Results obtained by them were quite high compared to what Brown and Ridley[1] reported. Also the interface energy values $\sigma_{\alpha\theta}$ obtained were too large. Hence the theory was rendered too complex to be implemented.

2.2 Interlamellar Spacing Criteria

The equation for the velocity of pearlite for bulk or interface diffusion-controlled growth does not give a unique solution for the growth rate, but rather a range of velocities and spacings which would satisfy the equation. In order to obtain a unique solution, a further condition needs to be imposed by using an optimization principle. There are mainly two different solutions reported for optimizing the interlamellar spacing.

2.2.1 Maximum growth rate

Zener's theory states that during pearlite growth the austenite-cementite and austenite-ferrite interfaces are bulging into the austenite phase due to capillarity effect, which reduces the composition difference responsible for driving the diffusion. Hence the effective composition difference gets reduced by a factor of $\left(1 - \frac{S_c}{S}\right)$ where S is the inter-lamellar spacing and S_c is the critical spacing at which the growth rate becomes zero. Zener suggested that the system selects the maximally growing velocity which can be obtained by differentiation of the velocity expression

along with the reduction factor with respect to S. This gives the relation $S = 2S_c$, where S_c is the critical inter-lamellar spacing at which growth stops.

2.2.2 Maximum rate of entropy production

The origin of this criteria is related to the thermodynamics of irreversible processes which deals with systems that are not in equilibrium but are in steady state. According to this theory the rate of energy dissipation is proportional to product of temperature and rate of entropy production ($\dot{S}$), i.e. $T\dot{S}$ which is given as:

$$T\dot{S} = JX \tag{2.10}$$

where J and X are the generalized flux and force respectively. Hence for an isothermal, isobaric and a unidirectional system:

$$\dot{S} = v\frac{\Delta G_v}{T} \tag{2.11}$$

where v is the transformation velocity and ΔG_v is the average Gibbs free energy per unit volume dissipated in the reaction. ΔG_v can be described as the difference between the maximum chemical free energy available and the surface energy accumulated.

$$\Delta G_v = \Delta G_v^0 - \frac{2\sigma}{S} \tag{2.12}$$

ΔG_v^0 can be approximated as

$$\Delta G_v^0 = \frac{\Delta H_v \Delta T}{T} \tag{2.13}$$

where ΔH_v is the latent heat evolved per unit volume and ΔT is the under-cooling. This allows us to express $\dot{S}$ as a function of S using the expressions for v derived earlier and G_v as follows:

$$\dot{S} = \beta \left(\frac{2\overline{D_v}}{S} \right) \frac{\Delta H_v \Delta T}{T_E T} \left(1 - \frac{S_c}{S} \right)^2 \tag{2.14}$$

where β contains the concentration terms. The maximum entropy production rate can be obtained by differentiating the above expression and equating to zero, which gives $S = 3S_c$ and $S = 2S_c$ for bulk and interface diffusion controlled mechanisms respectively.

Chapter 3

Analytical Model for Coupled growth

Pearlite is formed by redistribution of carbon form austenite to ferrite and cementite. It is essentially a coupled growth. We need a mathematical model which captures the physics of coupled growth and also gives freedom to control its properties. This chapter gives a review of the classical coupled growth analysis performed by Jackson and Hunt, which is used in our work to study pearlite transformation. Jackson and Hunt assumed a periodic composition profile for the growing front and solved it for the boundary conditions of coupled growth. The important mathematical detail has been included in the chapter. Subsequently, we use the analysis to understand growth under only interface diffusion and combined bulk and interface diffusion. The conclusion is that growth with only interface diffusion is not possible. Under mixed diffusion control the v vs λ curve for constant ΔT shifts up, which means that interface diffusion increases the growth velocity without affecting the lamellar spacing. The extent to which it shifts up depends on the interface diffusion constant or the interface mobility term.

3.1 Classical Jackson Hunt Theory

We have used the classical Jackson-Hunt analysis of eutectic solidification[7] to incorporate the necessary changes that occur in a solid state phase transformation. An understanding of the

original theory is critical to developing changes in the governing equation for implementation of interface diffusion. Solutions to coupled growth prior to Jackson and Hunt did not take care of the complete problem. Jackson and Hunt assumed a periodic composition profile at the interface and solved it for the governing equations. A summary of the analysis is provided here. The solution to the problem starts with a fourier series expansion of the composition which writes as follows

$$c = \sum_{n=-\infty}^{\infty} X_n e^{ik_n x - q_n y} + c^{\infty} \tag{3.1}$$

where x is the direction parallel to the interface and y is the growth direction. The relation between k_n and q_n can be obtained by solving the stationary diffusion equation for composition.

$$v\partial_y c + D\nabla^2 c = 0 \tag{3.2}$$

where $\partial_y c$ and $\nabla^2 c$ can be computed as follows

$$\frac{\partial c}{\partial y} = \sum_{n=-\infty}^{\infty} -q_n X_n e^{ik_n x - q_n y} \tag{3.3}$$

$$\nabla^2 c = \sum_{n=-\infty}^{\infty} q_n^2 X_n e^{ik_n x - q_n y} + \sum_{n=-\infty}^{\infty} -k_n^2 X_n e^{ik_n x - q_n y} \tag{3.4}$$

substituting the value of $\partial_y c$ and $\nabla^2 c$ in the governing equation we obtain

$$q_n^2 - \frac{v}{D} q_n - k_n^2 = 0 \tag{3.5}$$

which upon solving for q_n gives

$$q_n = \frac{v}{2D} + \sqrt{k_n^2 + \left(\frac{v}{2D}\right)^2} \tag{3.6}$$

For small values of peclet number ($\frac{v}{2D}$) the relation $q_n = |k_n|$ holds true. The stefan condition at the $\alpha-\gamma$ and $\theta-\gamma$ interface is used as boundary condition to get a solution for the composition profile. The stefan condition is given as follows

$$D\partial_n c_j = -v_n c_j^{\nu} \tag{3.7}$$

where $\partial_n c_j$ denotes the partial derivative of c_j in the direction normal to the interface and v_n is the normal velocity of the interface, D is the chemical diffusion coefficient and ν denotes the phase for which the condition is written. The details of the mathematics which leads to the final expression can be found in the original paper[7]. The final solution gives an expression for ΔT as a function of growth velocity v and the inter lamellar spacing(λ).

$$\Delta T = k_1 \left(\frac{v}{D}\lambda\right) + \frac{k_2}{\lambda} \tag{3.8}$$

where k_1 and k_2 are constants. A schematic of the relationship between ΔT, v and λ adopted from the original paper is shown in fig 3.1. It is important to note that for this analysis the average front temperature is taken to be equal for the growing phases which is an assumption. Our study is done under isothermal condition and hence this assumption hold good.

3.2 Theory for Interface diffusion

To implement the effect of interface diffusion in the transformation, the diffusion coefficient D is replaced with D_x and D_y with their respective laplacian terms, where D_x represents the interface diffusion coefficient and D_y represents the bulk diffusion coefficient. Hence the diffusion equation now reads as follows

$$v\frac{\partial c}{\partial y} + D_x\frac{\partial^2 c}{\partial x^2} + D_y\frac{\partial^2 c}{\partial y^2} = 0 \tag{3.9}$$

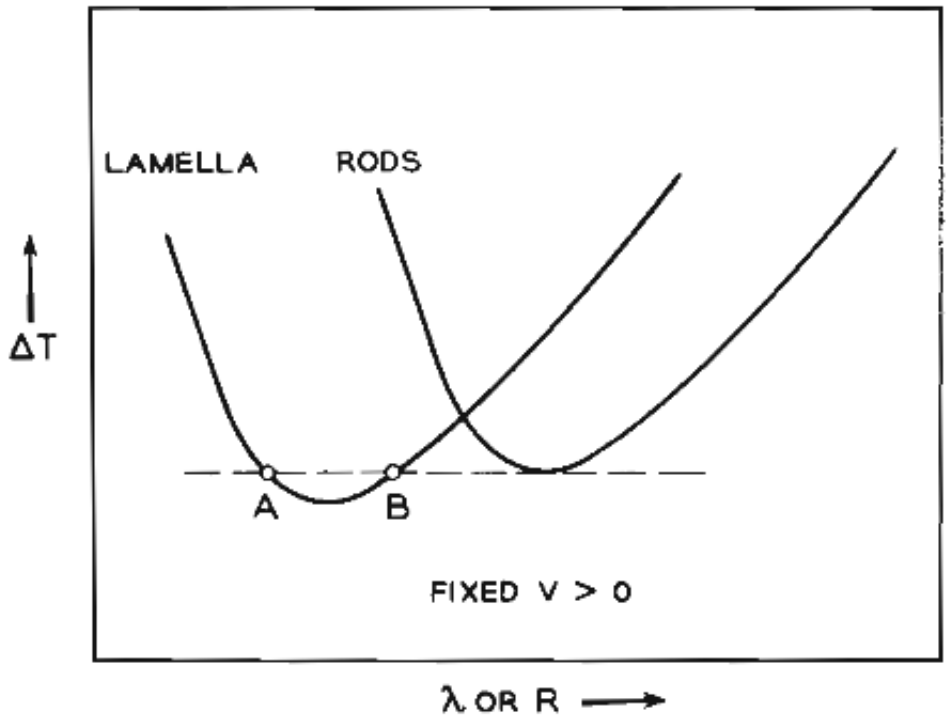

Figure 3.1: Schematic of ΔT vs λ curve adopted from the Jackson and Hunt's original paper

The modified relation between k_n and q_n is as follows

$$q_n^2 - \frac{v}{D_y} q_n - \frac{D_x}{D_y} k_n^2 = 0 \tag{3.10}$$

which yeilds

$$q_n = \frac{v}{2D} + \sqrt{\left(\frac{D_x}{D_y}\right) k_n^2 + \left(\frac{v}{2D}\right)^2} \tag{3.11}$$

Hence for small peclet number[] the relation between k_n and q_n modifies as

$$q_n = \sqrt{\frac{D_x}{D_y}} \, |k_n| \tag{3.12}$$

The stefan condition remains same and hence the remaining calculation does not change. The final equation for ΔT is as follows

$$\Delta T = k_1 \left(\frac{v}{\sqrt{D_x D_y}} \right) \lambda + \frac{k_2}{\lambda} \tag{3.13}$$

The above equation gives the effect of interface diffusion on ΔT and λ curve. It can be concluded that a particular combination of bulk and interface diffusion drives the pearlite reaction. It is also evident from eq 3.13 that growth by only interface diffusion is not possible as making D_x zero requires infinite under-cooling.

We define the ratio of interface to bulk diffusion constant as R, where $R = \frac{D_x}{D_y}$. The ΔT vs λ equation in terms of R is as follows.

$$\Delta T = k_1 \left(\frac{v}{\sqrt{R} D_y} \right) \lambda + \frac{k_2}{\lambda} \tag{3.14}$$

Under constant under-cooling the v vs λ equation is as follows

$$v = \frac{\sqrt{R} D_y}{k_1 \lambda} \left(\Delta T - \frac{k_2}{\lambda} \right) \tag{3.15}$$

This suggests that increasing interface diffusion or increasing the value of R will only shift the v vs λ profile up without affecting the lamellar-spacing.

Chapter 4

Numerical Model for Coupled growth

We use a grand potential multi-phase field model to simulate pearlite growth and study the effect of interface diffusion. Our model incorporates the thermodynamics of Fe-C binary system in a unique manner. We have used parabolic approximation for the free energies of the different phases. The cementite phase is a line compound and needs to be treated differently. This chapter describes the method of incorporation of the thermodynamics of Fe-C system in the phase-field model, followed by the details of the model itself. The details of the formulation of the model is provided in this chapter. The method of implementation of interface diffusion in the model is also described in detail.

4.1 Thermodynamic description of Fe-C system

Our model uses a unique method of incorporating the thermodynamics of Fe-C binary system in a phase-field model. It starts with the extraction of the G vs x data for different phases from thermodynamic databases. We have used thermo-calc to get G vs x data for austenite and ferrite phase and G vs T for cementite phase, as it is a line compound. Free energy densities are calculated by dividing the free energy values with molar volumes, which has been considered $10^{-6}m^3$ for all the phases. We have approximated the free energy densities of these phases using a second degree polynomial in composition. Parabolas are fit to the free energy curves of

the different phases at their respective compositions for different temperatures. The variation of the free energy with temperature is captured by the coefficients of the parabola which are assumed to be linear functions of temperature. This is done by fitting a straight line to the A, B and C values obtained at different temperatures. The above procedure is applicable to austenite and ferrite phases, however this does not work for cementite because the A value, which fixes the curvature of the parabola, is ideally infinite. This causes numerical issues during calculation of composition flux which is associated with the mobility term in the phase-field equation. Mobility is defined as

$$M = D\frac{\partial c}{\partial \mu} = \frac{D}{2A} = 0 \tag{4.1}$$

and hence vanishes for cementite. As a result it terminates the composition change for cementite and leads to numerical errors in the phase-field calculation. This necessitates the adoption of an alternate approximation technique for the implementation of cementite, which has been discussed in detail later. After the description of the free energy parameters of the different phases, the slopes and Gibbs-Thomson values are calculated. The surface energy values have been adopted from Sundquist's work[11].

4.1.1 Ferrite and Austenite Phase

As described above the free energy density of ferrite and austenite can be approximated as follows

$$f^{\alpha} = A^{\alpha}(T)c^2 + B^{\alpha}(T)c + C^{\alpha} \tag{4.2}$$

$$f^{\gamma} = A^{\gamma}(T)c^2 + B^{\gamma}(T)c + C^{\gamma} \tag{4.3}$$

where f^{α} and f^{γ} are the free energy per unit volume for ferrite and austenite phases respectively. For the ferrite phase parabolas are fit at the equilibrium compositions for the given temperature

but for austenite phase the parabola is fit at eutectoid composition at T_E for all temperatures as this phase is in equilibrium with both ferrite and cementite. Hence fitting the parabolas at one equilibrium composition will restrict the possibility of the other composition to be captured correctly. An example of the parabola fitting is shown for ferrite and cementite at $980K$.

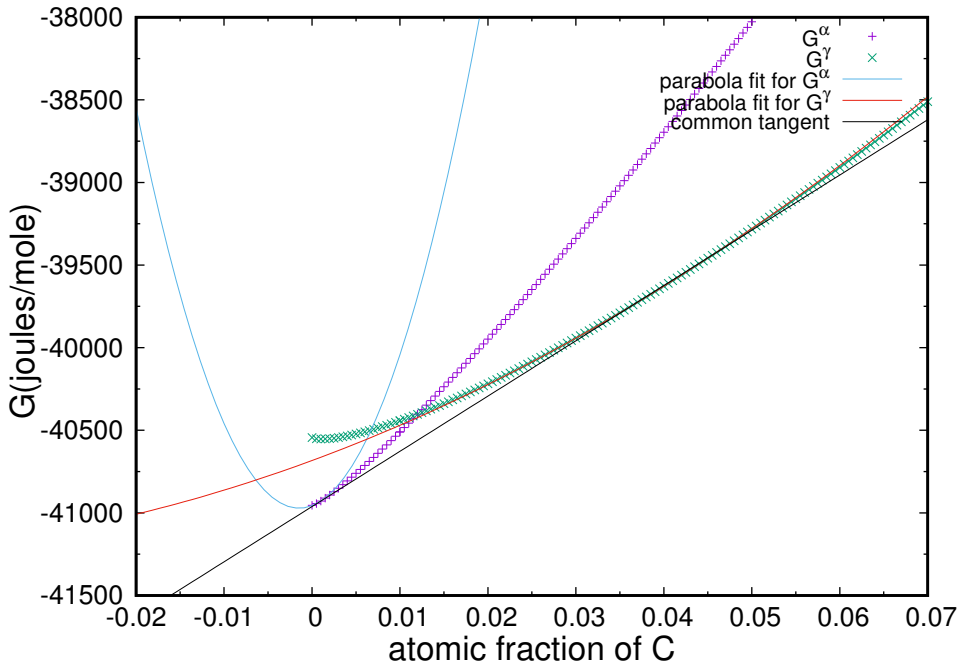

Figure 4.1: Parabola fit for ferrite and austenite phase at $980K$

Thereafter, the coefficients A, B and C are obtained from a linear interpolation of coefficients of parabola fit at the equilibrium compositions of respective phases at various temperatures. A linear fit of the parameters for austenite phase near T_E is shown in fig 4.2. These linear fits give the values of $\frac{\partial A}{\partial T}$, $\frac{\partial B}{\partial T}$ and $\frac{\partial C}{\partial T}$ for ferrite and austenite phases.

In the phase-field model the values of A, B and C for different phases are calculated as follows

$$A(T) = A_{T_{eq}} + \frac{\partial A}{\partial T}(T - T_{eq}) \tag{4.4}$$

$$B(T) = B_{T_{eq}} + \frac{\partial B}{\partial T}(T - T_{eq}) \tag{4.5}$$

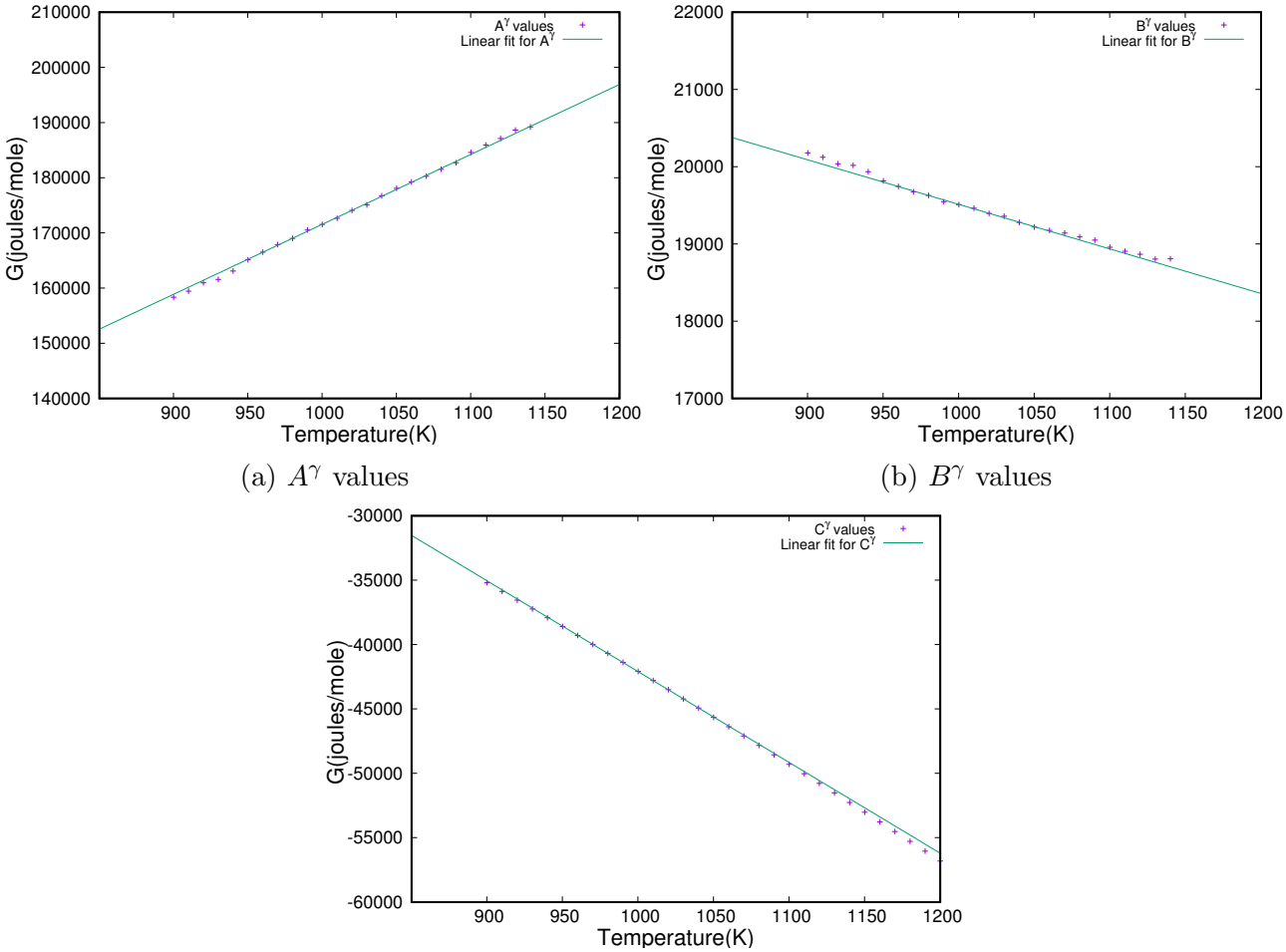

(a) A^{γ} values

(b) B^{γ} values

(c) C^{γ} values

Figure 4.2: Linear fit for A^{γ}, B^{γ} and C^{γ} near T_{eq}

$$C(T) = C_{T_{eq}} + \frac{\partial C}{\partial T}(T - T_{eq}) \tag{4.6}$$

These values are used to obtain important quantities like the slope(m), Gibbs-Thomsom coefficient(Γ), chemical potential(μ) and grand-potential(ψ)[3] which has been described later in detail. The phase-field model uses the grand-potential which is the Legendre transformation of free energy density. It is written as a function of μ. The equations are as follows.

$$\mu = \frac{\partial f}{\partial c} = 2Ac + B \tag{4.7}$$

$$\psi = f - \mu c = -Ac^2 + C = -\frac{(\mu - B)^2}{4A} + C \tag{4.8}$$

4.1.2 Implementation of Cementite

Cementite requires a different approach to capture the thermodynamics because it is a stoichiometric compound. The free energy vs composition curve of cementite phase can be approximated to be a extremely steep parabola which means that the curvature is infinite i.e. A^θ approaches infinity. This would mean that grand-potential density function for cementite phase, given by

$$\psi^\theta = -\frac{(\mu - B^\theta)^2}{4A^\theta} + C^\theta \tag{4.9}$$

is constant and equal to C^θ as the other term vanishes. One solution to this is to treat the free energy density of cementite phase as a point which is a function of temperature. The trace of the point is obtained in the form of G vs T data from CALPHAD shown in fig 4.3. The disadvantage of this method is that chemical potential at the point is not defined and hence $\frac{\partial c}{\partial \mu}$ vanishes. Therefore it needs an elegant approximation technique to capture the physics as well as reduce the complexity in the numerical model.

The idea is to have a constant finite curvature for cementite phase which can be kept several orders high than the curvature of the alpha phase to mimic the high curvature. This fixes the value of A^θ for cementite and subsequently the values of B^θ and C^θ can be obtained by equating the chemical potential and grand-potential respectively. It is worth noting that higher the value of A^θ we choose for cementite higher is the computation power required. In our model A^θ is fixed at one order higher than A^α which gives good results at reasonable computation time. B^θ and C^θ are determined using the following equations.

$$\mu^\gamma = \mu^\theta = \frac{\partial f^\gamma}{\partial c} = \frac{\partial f^\theta}{\partial c} = 2A^\gamma c + B^\gamma = 2A^\theta c + B^\theta \tag{4.10}$$

$$\psi^\gamma = \psi^\theta = -A^\gamma c_\gamma^2 + C^\gamma = -A^\gamma c_\gamma^2 + C^\theta \tag{4.11}$$

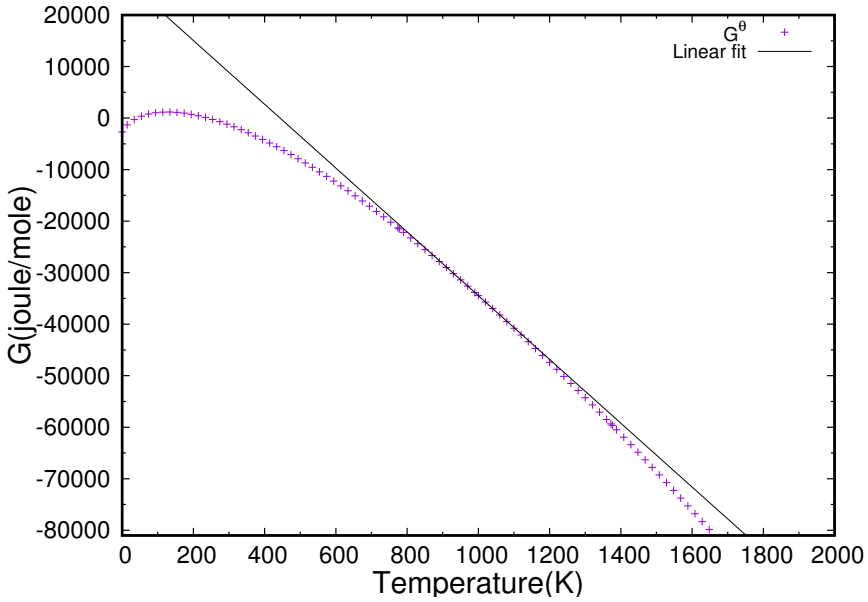

Figure 4.3: Linear fit for G

This fixes the value of B^θ and C^θ as a function of Temperature given by

$$B^\theta(T) = 2A^\gamma c_\gamma - 2A^\theta c_\theta + B^\gamma(T) \tag{4.12}$$

$$C^\theta(T) = A^\theta c_\theta^2 - A^\gamma c_\gamma^2 + C^\gamma \tag{4.13}$$

The values of $\frac{\partial B^\theta}{\partial T}$ and $\frac{\partial C^\theta}{\partial T}$ are obtained by differentiating the expressions for B^θ and C^θ as follows

$$\frac{\partial B^\theta}{\partial T} = \frac{\partial}{\partial T}(2A^\gamma c_\gamma - 2A^\theta c_\theta + B^\gamma) = 2c_\gamma \frac{\partial A^\gamma}{\partial T} + 2A^\gamma \frac{\partial c_\gamma}{\partial T} + \frac{\partial B^\gamma}{\partial T} \tag{4.14}$$

$$\frac{\partial C^\theta}{\partial T} = \frac{\partial}{\partial T}(A^\theta c_\theta^2 - A^\gamma c_\gamma^2 + C^\gamma) = -2A^\gamma c_\gamma \frac{\partial c_\gamma}{\partial T} - 2c_\gamma^2 \frac{\partial A^\gamma}{\partial T} + \frac{\partial C^\gamma}{\partial T} \tag{4.15}$$

The values for B^θ and C^θ depend on $\frac{\partial B^\theta}{\partial T}$ and $\frac{\partial C^\theta}{\partial T}$ which in turn depend on $\frac{\partial c_\gamma}{\partial T}$ i.e. $\theta - \gamma$ slope. Hence they are fixed by the choice of A^θ and $\theta - \gamma$ slope which essentially means that the B

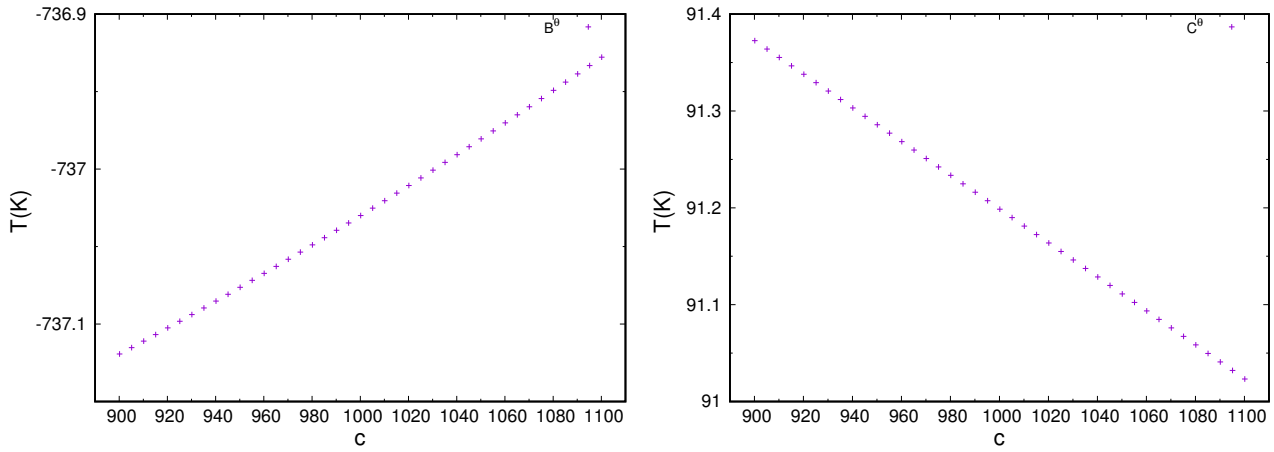

(a) B^θ values (b) C^θ values

Figure 4.4: B^θ and C^θ values obtained from eq 4.9 & 4.10

and C values may change but the equilibrium composition and the G values remain consistent with the original database values.

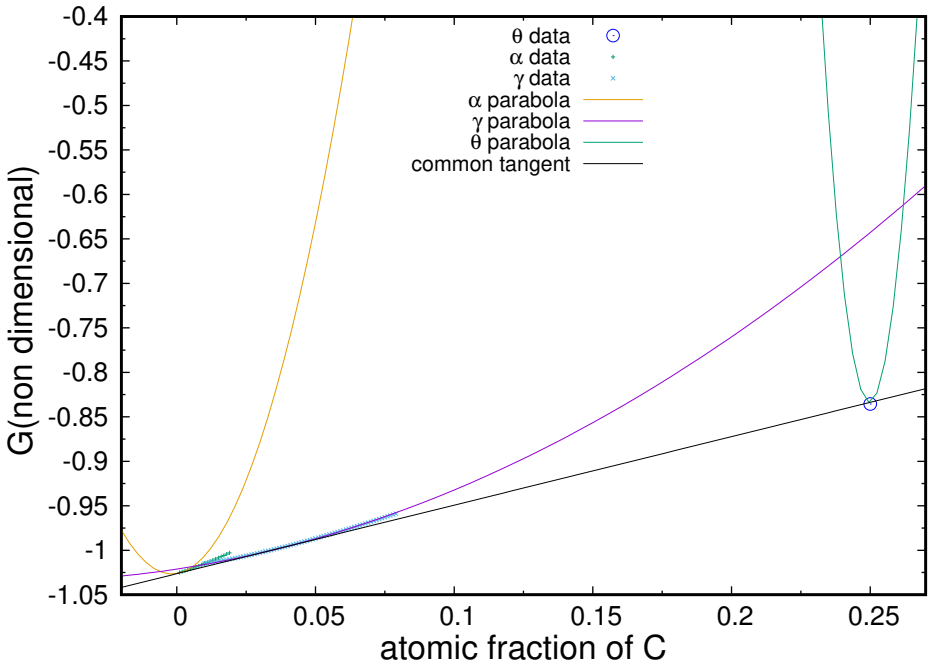

Figure 4.5: Example of a parabola fit for cememtite at T_{eq}

4.1.3 Gibbs Thomsom coefficient

Gibbs-Thomson coefficients for $\alpha-\gamma$ and $\theta-\gamma$ interfaces are very crucial parameters in the analysis of coupled growth of ferrite and cementite. These values must be accurately obtained for the correct description of the system. The Gibbs-Thomson coefficient between two phases are related to their grand-potential functions as follows

$$\Gamma^{1-2} = \frac{\sigma^{1-2}}{\left(\frac{\partial\psi^1}{\partial T} - \frac{\partial\psi^2}{\partial T}\right)} \tag{4.16}$$

where σ^{1-2} is the surface energy of interface. The Gibbs-Thomson coefficient for $\alpha-\gamma$ and $\theta-\gamma$ interfaces are determined by calculating $\frac{\partial\psi^\alpha}{\partial T}$, $\frac{\partial\psi^\theta}{\partial T}$ and $\frac{\partial\psi^\gamma}{\partial T}$ where ψ is expressed as a function of μ. The relations are as follows.

$$\frac{\partial\psi^\alpha}{\partial T} = \frac{(\mu - B^\alpha)}{2A^\alpha}\frac{\partial B^\alpha}{\partial T} + \frac{(\mu - B^\alpha)^2}{4(A^\alpha)^2}\frac{\partial A^\alpha}{\partial T} + \frac{\partial C^\alpha}{\partial T} \tag{4.17}$$

$$\frac{\partial\psi^\gamma}{\partial T} = \frac{(\mu - B^\gamma)}{2A^\gamma}\frac{\partial B^\gamma}{\partial T} + \frac{(\mu - B^\gamma)^2}{4(A^\gamma)^2}\frac{\partial A^\gamma}{\partial T} + \frac{\partial C^\gamma}{\partial T} \tag{4.18}$$

$$\frac{\partial\psi^\theta}{\partial T} = \frac{(\mu - B^\theta)}{2A^\theta}\frac{\partial B^\theta}{\partial T} + \frac{(\mu - B^\theta)^2}{4(A^\theta)^2}\frac{\partial A^\theta}{\partial T} + \frac{\partial C^\theta}{\partial T} \tag{4.19}$$

Once these quantities are obtained the Gibbs-Thomson coefficients for $\alpha-\gamma$ and $\theta-\gamma$ interfaces can be calculated as

$$\Gamma^\alpha = \frac{(\sigma^\alpha)}{\left(\frac{\partial\psi^\alpha}{\partial T} - \frac{\partial\psi^\gamma}{\partial T}\right)} \tag{4.20}$$

$$\Gamma^\theta = \frac{(\sigma^\theta)}{\left(\frac{\partial\psi^\theta}{\partial T} - \frac{\partial\psi^\gamma}{\partial T}\right)} \tag{4.21}$$

4.1.4 Fe-C binary Phase diagram

The procedure of fitting parabolas mentioned in the beginning of the chapter gives us temperature dependent free energy curves which can reproduce most of the thermodynamic properties like solidus and liquidus slopes, equilibrium composition, Gibbs-Thomson coefficient etc. The equilibrium co-existence lines for $\alpha - \gamma$ and $\theta - \gamma$ phases are obtained by the common tangent construction on the parabolas. This can be done by equating the chemical potential and grand-potential[3] of two variable points each on two different energy parabolas. The two equations combined together result in a quadratic equation which can be easily solved to get the equilibrium compositions. The phase diagram obtained by this method shown in fig [4.5] matches well with the original phase diagram.

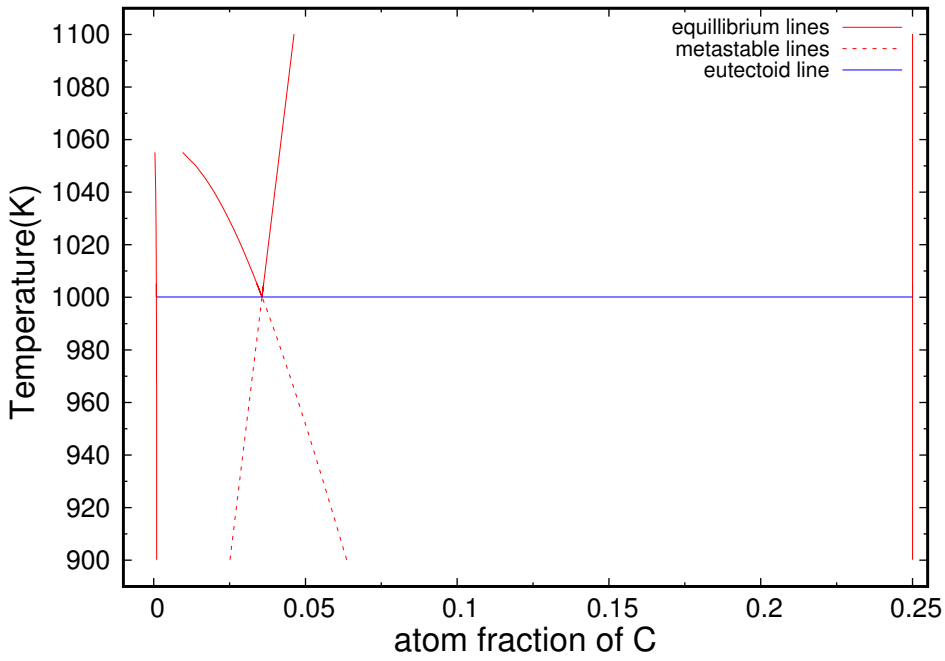

Figure 4.6: Phase diagram reproduced from parabolic approximation

The method of reproducing the properties of phase diagram for use in the phase-field model is consistent, however there are definite sources of error which can be safely neglected. The error percentage in the vicinity of equilibrium temperature, which actually is the region of our study,

Symbol	Value	Units
A^{γ}	1.7156×10^{11}	Jm^{-3}
A^{α}	6.0842×10^{12}	Jm^{-3}
A^{θ}	6.0842×10^{13}	Jm^{-3}
B^{γ}	1.9511×10^{10}	Jm^{-3}
B^{α}	2.0796×10^{10}	Jm^{-3}
B^{θ}	-3.0389×10^{13}	Jm^{-3}
C^{γ}	-4.2103×10^{10}	Jm^{-3}
C^{α}	-4.2312×10^{10}	Jm^{-3}
C^{θ}	3.7603×10^{12}	Jm^{-3}
$\partial_T A^{\gamma}$	1.2673×10^{8}	$Jm^{-3}T^{-1}$
$\partial_T A^{\alpha}$	-1.7985×10^{10}	$Jm^{-3}T^{-1}$
$\partial_T A^{\theta}$	0	$Jm^{-3}T^{-1}$
$\partial_T B^{\gamma}$	5.7671×10^{6}	$Jm^{-3}T^{-1}$
$\partial_T B^{\alpha}$	-4.0752×10^{7}	$Jm^{-3}T^{-1}$
$\partial_T B^{\theta}$	3.9497×10^{7}	$Jm^{-3}T^{-1}$
$\partial_T C^{\gamma}$	-7.0541×10^{7}	$Jm^{-3}T^{-1}$
$\partial_T C^{\alpha}$	-6.700×10^{7}	$Jm^{-3}T^{-1}$
$\partial_T C^{\theta}$	$-7.1995 \times 10^{7}7$	$Jm^{-3}T^{-1}$
c^{α}	8.8×10^{-4}	-
c^{β}	0.25	-
c^{γ}	0.03431	-
η_{α}	0.865	-
η_{β}	0.135	-

Table 4.1: Thermodynamic Parameters for pearlite obtained from CALPHAD

is significantly small and hence validates our analysis.

4.2 Phase field model

4.2.1 Multi-phase field model

As discussed in introduction a phase-field model is a mathematical model used for solving interfacial problems like viscous fingering, solidification dynamics, fracture dynamics, vesicle dynamics and so on. The material under study generally comprises multiple phases and components e.g. Fe-C system. Phase-field study of two phase systems is fairly simple where a single order parameter is sufficient to describe all the phases e.g. solidification of pure Aluminum. However multi-component and multi-phase systems are complex and require simultaneous treatment of all the phases, where more than one order parameter is necessary. Multi-phase field models have been developed to treat this class of problems where more than two phases are involved.

We have used a grand potential multi-phase field model recently developed by Choudhury and Nestler[3]. In this section, we review the basics of a multiphase field model which has been implemented in our model. We consider a system of N phases where each phase α is denoted by an order parameter ϕ_α which is continuous throughout the domain. The state of a phase α is represented by ϕ_α whose value lies between 0 and 1. The order parameter is a function of space and its value denotes the presence or absence of that phase. A value of unity implies that the region consists of the bulk phase. Similarly a fractional value of the order parameter denotes partial presence of that phase which means that the region contains the interface. At any region the sum of all the order parameters must be unity which can be represented as $\sum_{\alpha=1}^{N} \phi_\alpha = 1$.

In the multi-phase field model[3], the grand potential density functional(Ω) can be expressed

as follows

$$\Omega\left(\mu, T, \phi\right) = \int_V \left[\Psi\left(\mu, T, \phi\right) + \left(\epsilon a(\phi, \nabla\phi) + \frac{1}{\epsilon} w\left(\phi\right)\right)\right] dV \tag{4.22}$$

where $\phi = [\phi_1, \phi_2, \cdots, \phi_N]$ are the phase-fields representing the spatial arrangement of N phases and $\mu = [\mu_1, \mu_2, \cdots, \mu_{K-1}]$ are the diffusion potentials associated with each one of the $K-1$ independent solutes.The functionals w and a represent the surface potential and the gradient energy density respectively. The minimization of Ω leads to the evolution of the spatial arrangement of the phases (ϕ) denoted by,

$$\tau\epsilon\frac{\partial\phi_\alpha}{\partial t} = \epsilon\left(\nabla\cdot\frac{\partial a(\phi,\nabla\phi)}{\partial\nabla\phi_\alpha} - \frac{\partial a(\phi,\nabla\phi)}{\partial\phi_\alpha}\right) - \frac{1}{\epsilon}\frac{\partial w\left(\phi\right)}{\partial\phi_\alpha} - \frac{\partial\Psi\left(\mu,T,\phi\right)}{\partial\phi_\alpha} - \Lambda \tag{4.23}$$

where τ is the relaxation constant with its value set based on the criterion stated in [3] to obtain a diffusion controlled interface motion and Λ is the lagrange parameter used to ensure $\sum_{\alpha=1}^{N}\phi_\alpha = 1$ at every mesh point in the simulation domain. Let the right hand side of Eq. 4.24 except Λ term be denoted as E_α. Now Λ can be derived from the constraint condition $\sum_{\alpha=1}^{N}\phi_\alpha = 1$ which gives

$$\sum_{\alpha=1}^{N}\frac{\partial\phi_\alpha}{\partial t} = \sum_{\alpha=1}^{N}\left(E_\alpha - \Lambda\right) = 0$$

hence

$$\Lambda = \frac{1}{N}\sum_{\alpha=1}^{N} E_\alpha. \tag{4.24}$$

The gradient energy density $a\left(\phi, \nabla\phi\right)$ for an isotropic case can be written in terms of a generalized antisymmetric gradient vector

$$a(\phi,\nabla\phi) = \sum_{\alpha=1,\beta=1,\alpha<\beta}^{N,N}\gamma_{\alpha\beta}\left|q_{\alpha\beta}\right|^2 \tag{4.25}$$

where, $\gamma_{\alpha\beta}$ is the $\alpha-\beta$ interface energy, and $q_{\alpha\beta}$ is the normal vector to the $\alpha-\beta$ interface, written as $q_{\alpha\beta} = \phi_\alpha\nabla\phi_\beta - \phi_\beta\nabla\phi_\alpha$. The surface potential $w(\phi)$ is chosen as a double-obstacle

potential over double-well potential. The advantage in double-obstacle potential is that the partial differential equations only need to be solved at certain places so it is computationally efficient. The potential $w(\phi)$ writes as

$$w(\phi) = \frac{16}{\pi^2} \sum_{\substack{\alpha,\beta=1 \\ (\alpha<\beta)}}^{N,N} \gamma_{\alpha\beta}\phi_\alpha\phi_\beta + \sum_{\substack{\alpha,\beta,\delta=1 \\ (\alpha<\beta<\delta)}}^{N,N,N} \gamma_{\alpha\beta\delta}\phi_\alpha\phi_\beta\phi_\delta \tag{4.26}$$

where the higher order term $\gamma_{\alpha\beta\delta}\phi_\alpha\phi_\beta\phi_\delta$ is added to maintain the solution at an $\alpha-\beta$ interface strictly along the two phase interface. The value of $\gamma_{\alpha\beta\delta}\phi_\alpha\phi_\beta\phi_\delta$ is chosen to be $\approx 10\gamma_{\alpha\beta}$. But, ϕ_α can take any value if we do not impose the criteria that $w(\phi)$ is valid only within a domain, elsewhere it is infinity. So we define a Gibbs simplex $\sum = \{\phi \,|\, \sum_{\alpha=1}^{N} \phi_\alpha = 1 \text{ and } \phi_\alpha \geq 0\}$ which is imposed to correct the ϕ_α values after each time evolution step.

In this model the driving force for transformation is represented by the difference in the grand potentials between two phases α and β as

$$\Delta\Psi^{\alpha\beta} = \Psi^\alpha - \Psi^\beta \tag{4.27}$$

The grand-potentials of the individual phases is given by

$$\Psi^\alpha = f^\alpha(\mathbf{c}^\alpha(\mu,T),T) - \sum_{i=1}^{K-1} \mu_i c_i^\alpha(\mu,T). \tag{4.28}$$

All the grand-potentials of the participating phases (Ψ^p)'s at any particular point in the simulation domain are interpolated to obtain Ψ as,

$$\Psi(\mu,T,\phi) = \sum^{\alpha} \Psi^\alpha(T,\mu) h_\alpha(\phi) \tag{4.29}$$

where

$$h_\alpha(\phi) = \phi_\alpha^2 \left(3 - 2\phi_\alpha\right) + 2\phi_\alpha \sum_{\substack{m=1,n=1,\\ m<n,m\neq\alpha,n\neq\alpha}}^{N,N} \phi_m \phi_n \tag{4.30}$$

where $h_\alpha(\phi)$ interpolates between all the phases and also satisfies $\sum_{\alpha=1}^{N} h_\alpha(\phi) = 1$. The evolution of μ for multi-phase field model is calculated for each component, where the mobility is taken as a weighted value of mobility in all the phases. The μ evolution equation is expressed as follows:

$$\left\{\frac{\partial \mu_i}{\partial t}\right\} = \left[\sum_\alpha h_\alpha\left(\phi\right) \frac{\partial c_i^\alpha\left(\mu, T\right)}{\partial \mu_j}\right]_{ij}^{-1} \left\{\nabla \cdot \left(\sum_{j=1}^{K-1} M_{ij}\left(\phi\right) \nabla \mu_j - \mathbf{J}_{at,i}\right) - \sum_\nu c_i^\alpha\left(\mu, T\right) \frac{\partial h_\alpha\left(\phi\right)}{\partial t}\right\}_j \tag{4.31}$$

where i and j iterate over the $(K-1)$ independent components. $[\cdot]$ denotes a matrix of dimension $((K-1)\times(K-1))$ while $\{\cdot\}$ represents a vector of dimension $(K-1)$. The anti-trapping current $\mathbf{J_{at,i}}$ has a sense and magnitude which nullifies solute trapping at the solid-liquid interface and is determined by the expressions given in[3]. The atomic mobility, $M_{ij}\left(\phi\right)$ is obtained by interpolating the individual phase mobilities as,

$$M_{ij}\left(\phi\right) = \sum_\nu M_{ij}^\alpha g_\alpha(\phi) \tag{4.32}$$

and each of the M^α is related to diffusivity as

$$M_{ij}^\alpha = D_{ik}^\alpha \left(\frac{\partial c_k^\alpha(\mu, T)}{\partial \mu_j}\right) \tag{4.33}$$

4.2.2 Implementing Interface Diffusion

Interface diffusion is incorporated in our model by adding an interface mobility term to bulk mobility in the evolution equation as follows.

$$\frac{\partial \mu}{\partial t} = \nabla.\left[(M_{bulk} + M_{interface})\nabla\mu\right] + \quad other \quad terms \tag{4.34}$$

It is assumed that interface diffusion occurs only in a small region near to the $\alpha - \gamma$ and $\theta - \gamma$ interfaces. In our model the interface regions are denoted by fractional order parameter for all the phases and bulk region is associated with order parameter of 1 for that phase and 0 for the rest of the phases. The products $\phi_\alpha\phi_\gamma$ and $\phi_\theta\phi_\gamma$ take positive values in the interface and 0 everywhere else in the domain. This is used to restrict the bulk and interface mobility terms to their respective regions. So we multiply ϕ_i to bulk mobility and $\phi_i\phi_j$ to interface mobility. The relation can be expressed as follows

$$M = \sum_i M_{bulk}\phi_i + \sum_{i<j} M_{interface}\phi_i\phi_j \tag{4.35}$$

Chapter 5

Results and Discussion

Analytical calculations detailed in chapter [3] suggests that interface diffusion increases the growth velocity, without affecting the inter-lamellar spacing. In chapter [4] we lay the foundation of our numerical model for the investigation of the above prediction. Precisely, we elucidate the thermodynamic description and the mathematical details of the model. In this chapter, we use the model to simulate pearlite growth with both bulk and interface diffusion. The model is validated initially by running simulation for a demo system. We choose a hypothetical symmetric system with non-dimensional parameters for benchmarking. The results support the analytical formulation for interface diffusion described in chapter [3]. Subsequently, we incorporate the thermodynamic data for Fe-C binary system in our model as described in chapter [4]. First, we study the growth behavior of pearlite with only bulk diffusion. The details of the simulation parameters can be found in this chapter. Thereafter, simulations are run with increasing values of interface diffusion. The results obtained further strengthen our hypothesis based on analytical equation that interface diffusion raises the v vs λ curve without affecting the lamellar-spacing. We also study the effect of interface diffusion on phase fractions during growth and the dependence of velocity on the ratio of interface to bulk mobilities(R).

5.1 Qualitative analysis with symmetric system

Before implementing the thermodynamics of pearlite discussed in section [4.1], the model is verified for a demo system. We take a hypothetical symmetric system with non-dimensional parameters as mentioned in Table. [5.1]. The free energy curves of the phases for this system are extrapolated from the chosen values of equilibrium composition and slopes. As described in the previous chapter the free energy curves are taken as parabolas. The curvature of the parabolas and the diffusivity is taken as unity. The differential equations are discretized using finite difference method and solved using multi-grid technique with periodic boundary conditions. The grid size is set by Δx and Δy, with $\Delta x = \Delta y = 2$ and time step is kept 0.2 for this simulation. The relaxation parameter τ is calculated in the model as per the criterion given in [3]. The parameter ϵ is related to the interface width which should be taken small enough to reproduce the real conditions but should also be large enough to have adequate no of grid points in the interface to avoid singularities. Ideally it's value is set four times Δx. The mesh size in the x direction must be equal to the λ we want to set for the simulation and in the y direction it can take any value. The domain is initialized with the equilibrium compositions and volume fractions as chosen in the demo system shown in Table [5.1]. After setting the domain parameters, the simulation is run with the given under-cooling until it equilibrates. Fig. [5.1] shows the domain at $t = 0$ and $t = 10000$.

The initial velocity of the system is set at a high value but after each time step it takes the value decided by the governing equation until it reaches steady state where the average velocity remains constant. The velocity of growth for a particular simulation is calculated by taking the average of the last few velocities after the system has equilibrated. For the demo system this occurs at around 2 lacs time steps.

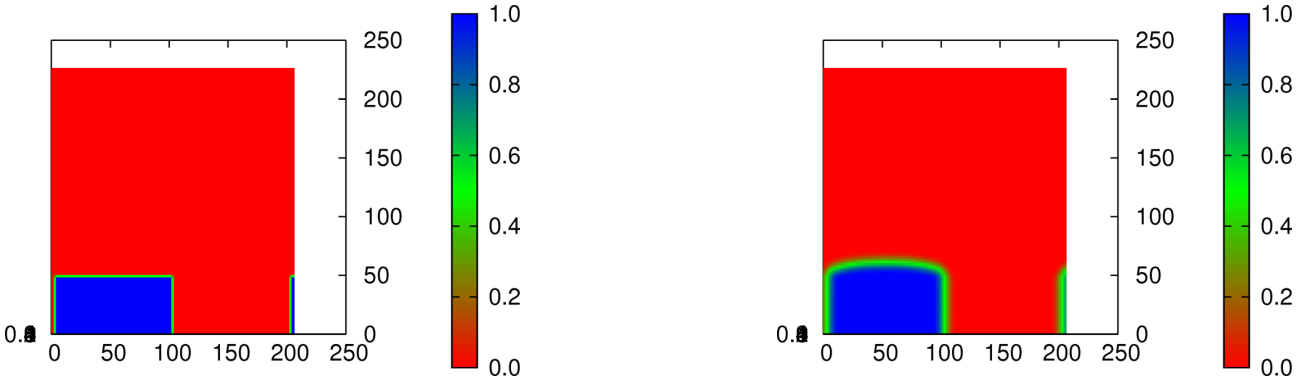

(a) (b)

Figure 5.1: (a) and (b) shows ϕ profile for α phase at times 0 and 10^3 steps

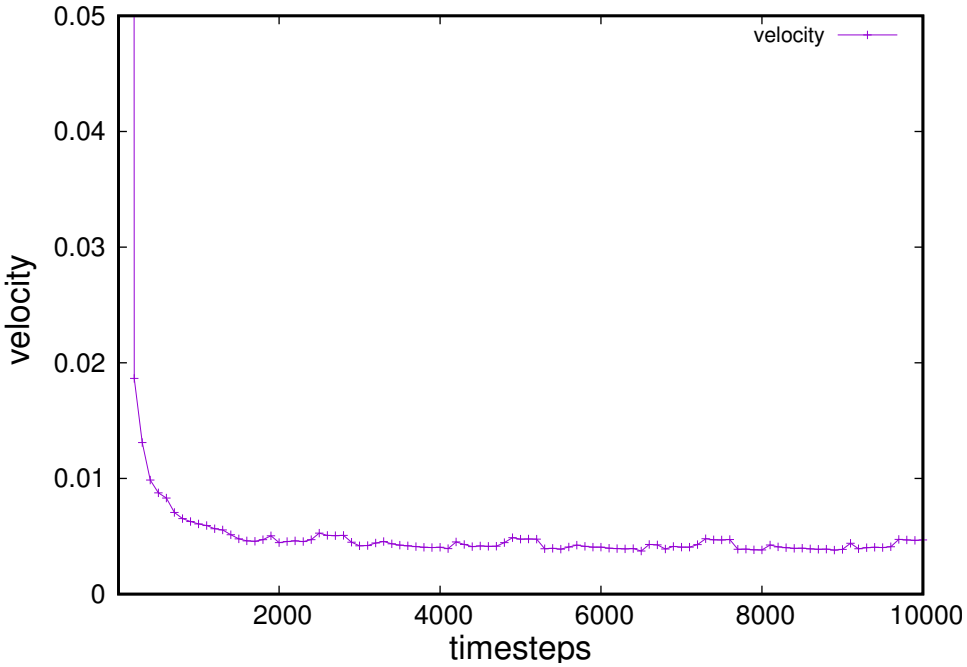

Figure 5.2: Saturation of growth velocity with increasing time steps

Simulations are performed using our model with the given parameters of the demo system to obtain a close match with the analytical curve as shown in Fig. [5.3]. The growth velocity until 10000 time steps is shown in Fig. [5.2].

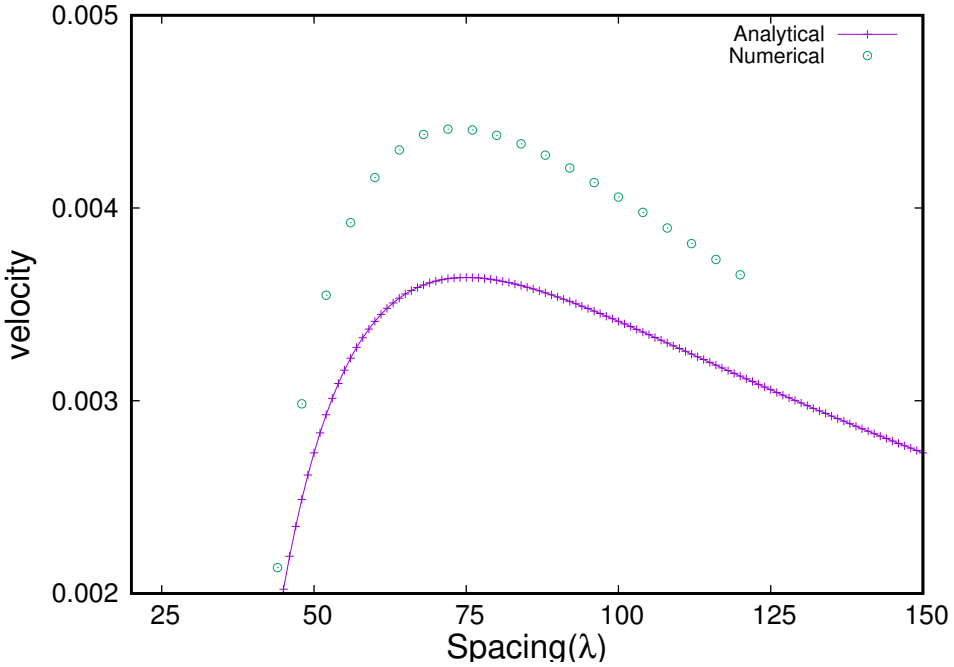

Figure 5.3: Plot of numeric and analytical v vs λ profile for symmetric system

The numerical curve lies above the analytical curve, within the tolerance range of 20%, also it predicts the maximally growing λ correctly. Thereafter, we introduce interface mobility in terms of R and run the simulations for increasing values of R. This gives a qualitative effect of introduction of interface mobility in coupled growth as shown in Fig. [5.4].The phase field simulation results agree to what is predicted by the analytical model. The velocity profile just moves up with increasing interface mobility.

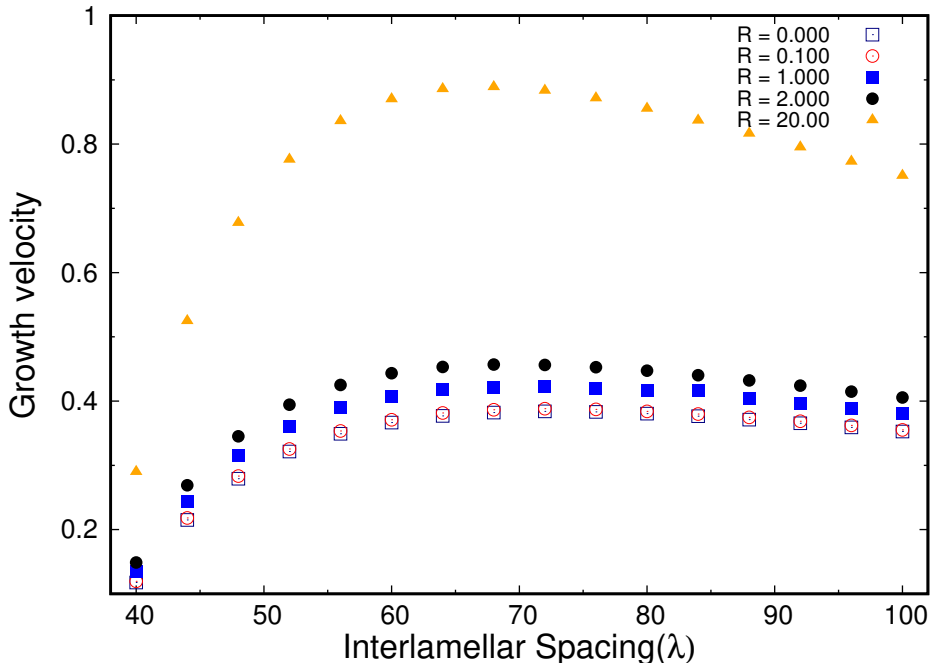

Figure 5.4: v vs λ for increasing values of R

Symbol	Value	Units
T_E	1.0	-
ΔT	0.04	-
$\sigma^{\alpha\gamma} = \sigma^{\beta\gamma} = \sigma^{\alpha\beta}$	1.0	-
D^{γ}	1.0	-
c^{α}	0.2	-
c^{β}	0.8	-
c^{γ}	0.5	-
η_{α}	0.5	-
η_{β}	0.5	-
$\theta_{\alpha\beta} = \theta_{\beta\alpha}$	30°	degrees
$A_{\alpha} = A_{\beta} = A_{\gamma}$	1.0	-
m_{α}	-0.45	-
m_{β}	0.45	-

Table 5.1: Parameters used for analytical calculation of symmetric system

5.2 Pearlite growth with bulk diffusion

The analysis with the symmetric system gives consistent results as expected from the analytical calculation. In this section we describe the integration of thermodynamics of Fe-C system into multi-phase field model to simulate pearlite growth with only bulk diffusion. We start with the introduction of the energy parabolas for ferrite, cementite and austenite phase into the model as described in Section [4.1]. The curvature of cementite parabola is set one order higher than ferrite phase. The Gibbs-Thomson coefficient is calculated using the grand potentials and the interface free energy, which is taken as $0.7Jm^{-2}$ based on Sundquist's work[11]. The equilibrium compositions, volume fractions and slopes as obtained from the free energies are set in the model. We have assumed volume diffusion only in the austenite phase, hence the bulk diffusivity in ferrite and cementite phases are set to 0. The bulk diffusivity for austenite phase is taken as $10^{-9}m^2/s$. All the thermodynamic parameters are non-dimensionalized using proper references. The free energies densities are calculated with respect to the austenite free energy density at T_{eq}. The temperature is used with respect to T_{eq}. The length-scale is derived from the ratio of surface energy to austenite free energy density at T_{eq}. The time-scale is chosen with respect to length-scale such that the diffusivity becomes unity. The remaining parameters are calculated from these scales. All the parameters used is shown in Table. [5.2].

This simulation is done at an under-cooling of 20K. The analytical equation predicts the maximally growing spacing for the given parameters as 1914.5 length units(non-dimensional). Hence we have chosen $\Delta x = \Delta y = 15.0$ to allow sufficient simulation points for the $\alpha - \theta$ interface in the domain. So the grid size in x direction(MESHX) corresponding to maximally growing spacing is set as 127.63 and in y direction as 200. The time step(Δt) is taken 0.225. The τ and ϵ values are enumerated in Table. [5.2], calculated as described before in Section. [5.1]. Fig. [5.5] shows the growth of pearlite for MESHX = 144 at different time steps.

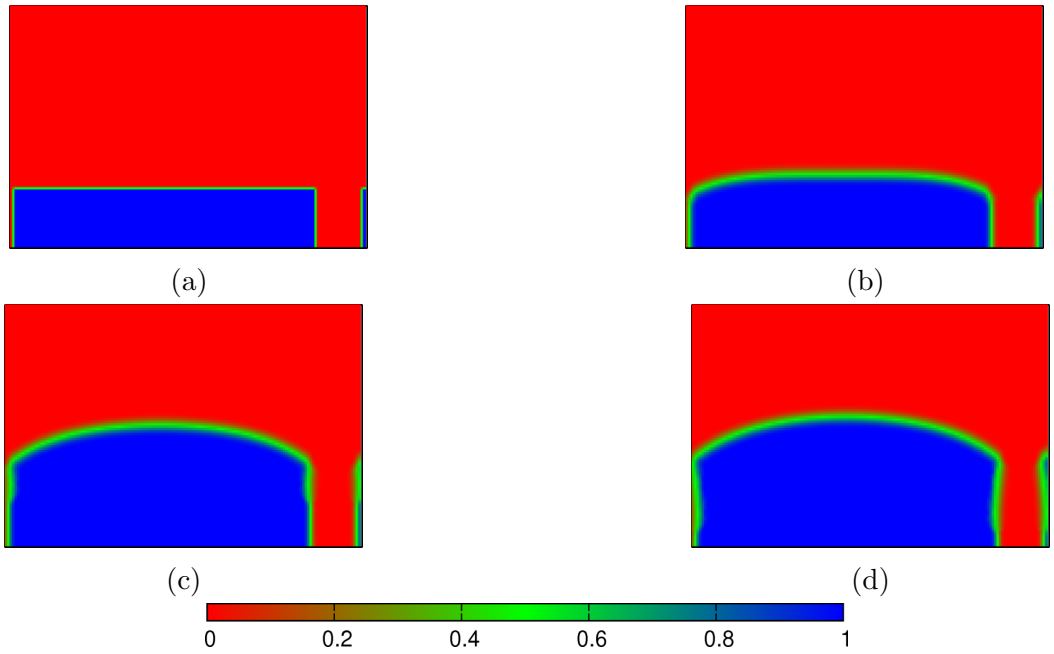

Figure 5.5: (a), (b), (c), (d) show growth of pearlite at time steps 0, 10^6, 10^7 and 2×10^7 steps

The v vs λ profile is generated by running simulations for several points on either side of the maximally growing wavelength obtained from analytical equation as shown in Fig. [5.6]. The maximally growing v and λ predicted by phase field is off from analytical prediction. Slight deviations in the phase-field model results are expected to occur which may have arose from the errors during linearization of A, B and C parameters. However the error values are within 20%, which is the safe limit to ensure validity of our analysis. The errors reduce as we do simulations closer to T_{eq}.

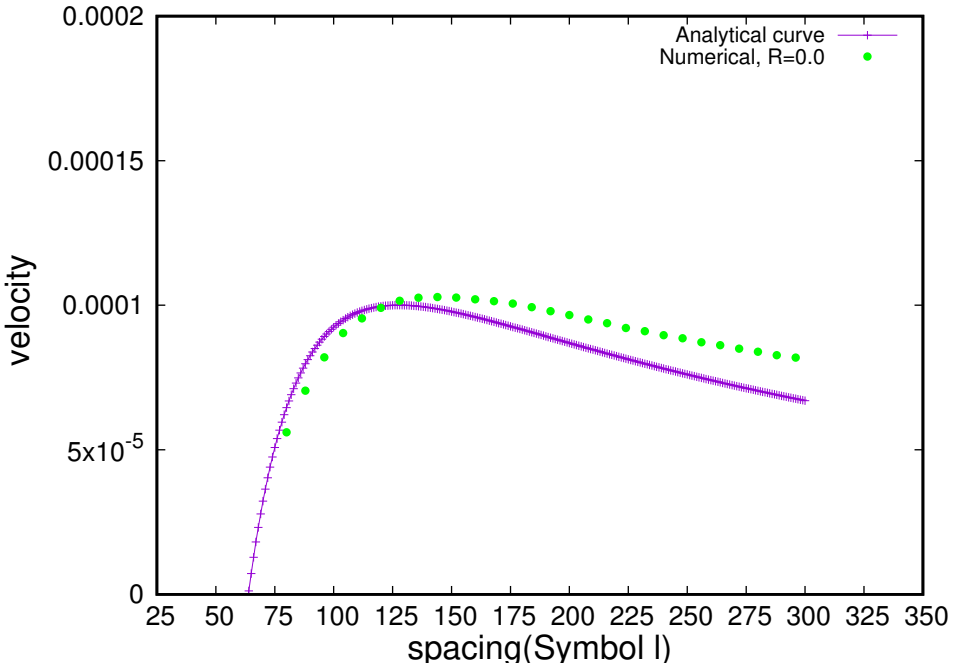

Figure 5.6: Plot of numeric and analytical v vs λ profile

Symbol	Value	Units
T_{eq}	1000.15	K
ΔT	20	K
$\sigma^{\alpha\gamma} = \sigma^{\beta\gamma} = \sigma^{\alpha\beta}$	0.7	J/m^2
D^{γ}	1×10^{-12}	m^2/s
c^{α}	8.8×10^{-4}	-
c^{β}	0.25	-
c^{γ}	0.03431	-
η_{α}	0.865	-
η_{β}	0.135	-
$\tau_{\alpha\gamma}$	$1.704103e+08$	-
$\tau_{\theta\gamma}$	$7.093866e+09$	-
$\Delta x = \Delta y$	15.0	-
$\theta_{\alpha\beta} = \theta_{\beta\alpha}$	30°	degrees

Table 5.2: Parameters used for analytical calculation and phase-field model

5.3 Effect of interface diffusion on Pearlite transformation

In the previous chapter we successfully simulate pearlite growth with only volume diffusion. Results similar to qualitative analysis performed in section [5.1] is expected upon addition of interface mobility. With this idea, we introduce interface mobility to our model as described in section [4.2.2]. The remaining simulation parameters used in the present case is same as used in section [5.2] given in table [5.2]. All the simulations are run for 2×10^7 steps. In this section we describe the effect of interface diffusion obtained from our simulations broadly under the following headings

1. Effect of average interface mobility on pearlite growth in terms of changes in v vs λ profile.
2. Effect of asymmetric mobilities on v vs λ profile and phase fractions.
3. Dependence of maximally growing velocity on ratio of interface to bulk mobilities.

5.3.1 Pearlite growth under interface diffusion

The term M_{gb} denotes the average mobility which is calculated as the volume fraction average of the two interfaces. M_{gb} is expressed as

$$M_{gb} = \eta_\alpha M_\alpha + \eta_\theta M_{theta} \tag{5.1}$$

where η_α and η_θ denote the volume fraction of ferrite and cementite phase respectively. M_α and M_θ are the corresponding interface mobilities. In this simulation we take equal mobilities for $\alpha - \gamma$ and $\theta - \gamma$ interfaces. Hence

$$Mgb = M_\alpha = M_\theta$$

The bulk mobilities for the phases are of the order of 10^{-3}(non-dimensional).The interface mobility for both the phases are set few orders higher than bulk mobility for this study. The remaining simulation parameters are same as that used in section [5.2]. Next, simulations are run to obtain the v vs λ curve for average interface mobilities of 0.1 and 1.0 as shown in Fig. [5.8]. Pearlite growth with interface mobility 1.0 at an under-cooling of 20K for different times is shown in Fig. [5.7].

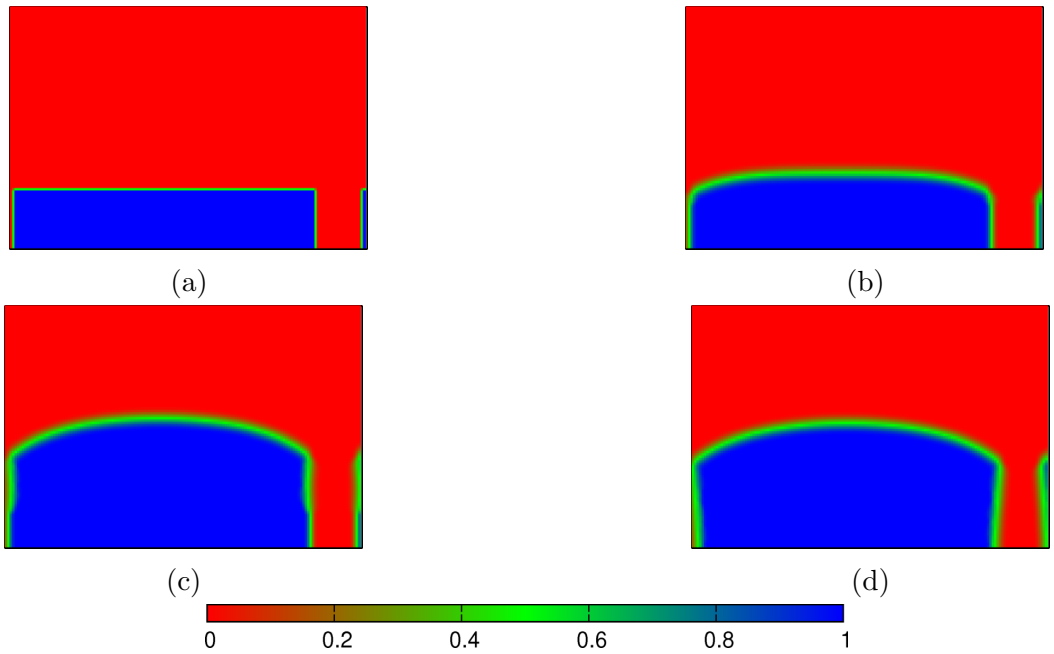

Figure 5.7: (a), (b), (c), (d) show growth of pearlite with interface diffusion at time steps 0, 10^6, 10^7 and 2×10^7 steps. $MESHX = 144$, $\Delta T = 20$

As expected the velocity profile shifts up without any change in the maximally growing wavelength. This is in line with our hypothesis based on the analytical calculation performed in chapter [3]. It can be safely concluded that interface mobility does not play a role in the selection of the inter-lamellar spacing but only increases the diffusion rate and hence the growth velocity. A comparison of Fig [5.5] and Fig [5.7] shows that the system with interface mobility grows faster and thus reaches equilibrium earlier. All the simulations have been run for the same time. So the system with maximum interface mobility has taken the form of the analyt-

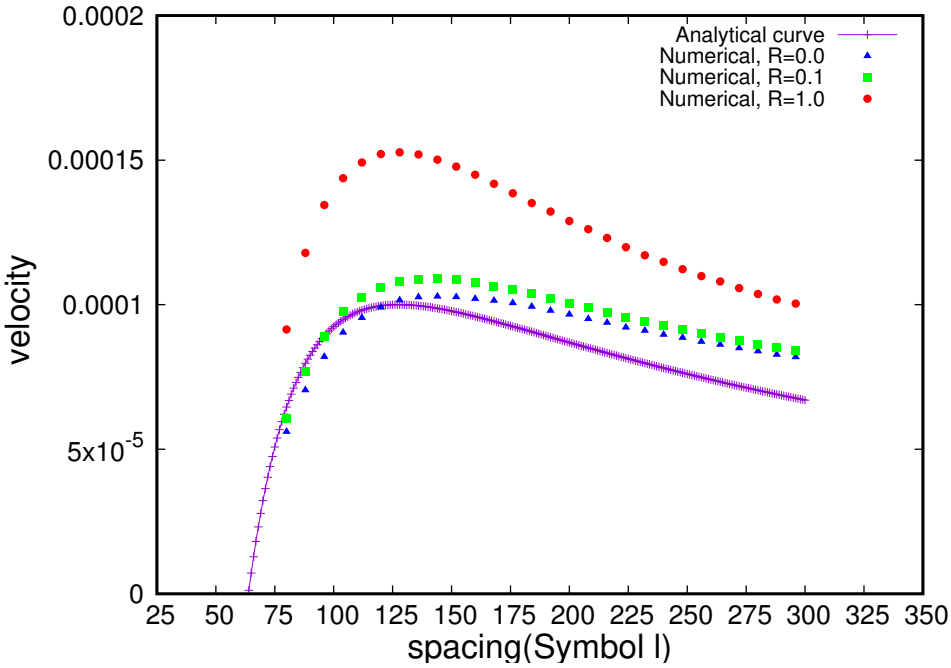

Figure 5.8: Plot of numeric v vs λ profiles for different ratios of interface to bulk mobilities

ical equation best as evident from Fig [5.8], which explains the difference in the form of the curves. Given enough time all the curves will take the form of the analytical curve. Solid state transformations at lower under-coolings are significantly slower that eutectic transformations, hence our simulations relatively time-expensive.

5.3.2 Effect of asymmetric mobilities of ferrite and cementite

Equal interface mobilities for ferrite and cementite is an assumption. In reality the interface mobilities are expected to be different, owing to their different structural properties. However the exact difference in the mobilities are unknown. In this section we simulate pearlite growth with different ratios of cementite to ferrite mobilities keeping the volume fraction average mobility M_{gb} constant. Let r be the ratio of cementite to ferrite mobility expressed as

$$r = \frac{M_\theta}{M_\alpha}$$

The constraint of constant volume fraction average mobility gives

$$M_\alpha + M_\theta = M_{gb}$$

Hence for a given ratio r the individual mobilities can be calculated as

$$M_\alpha = \frac{M_{gb}}{1+r} \tag{5.2}$$

and

$$M_\theta = \frac{rM_{gb}}{1+r} \tag{5.3}$$

We take $M_{gb} = 1.0$ and obtain v vs λ curve for $r = 0.05$, 2 and 20 as shown in Fig [5.9]. For $r = 2$, the velocity profile just begins to shift down, which indicates that asymmetric mobilities reduces growth velocity. The reduction in velocity is significant when asymmetry is high, $r = 20$. For the opposite asymmetry i.e. for $r = \frac{1}{20}$, the reduction is significant but not as much as the previous case. This suggests that $\alpha - \gamma$ interface is more dominant in controlling interface diffusion which can be attributed to its higher volume fraction compared to $\theta - \gamma$ interface.

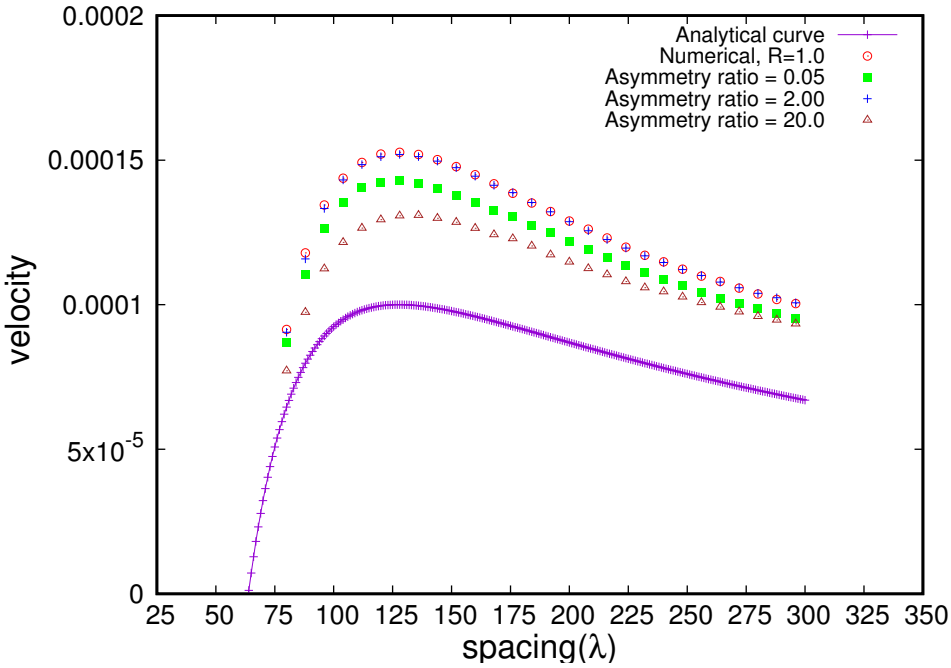

Figure 5.9: Plot of numeric v vs λ profiles for different ratios of cementite to ferrite interface mobilities

5.3.3 Dependence of velocity on interface Diffusion

The analytical calculation done in section 3.2 predicts that growth velocity is proportional to the square root of R which is the ratio of interface to bulk diffusivity. This is evident from equation 3.15 given as

$$v = \frac{\sqrt{R}D_y}{k_1\lambda}\left(\Delta T - \frac{k_2}{\lambda}\right)$$

Fig. [5.10] shows the dependence of v^2 on R as obtained from simulations. It is clear that square of velocity is almost proportional to R which suggests that our simulations are in line with our analytical calculations.

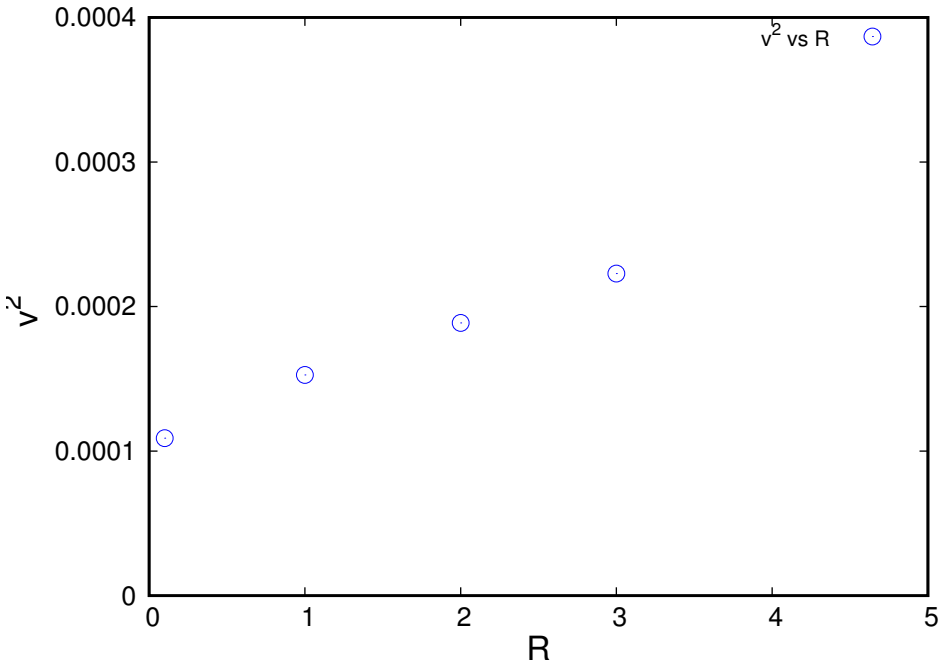

Figure 5.10: Plot of v^2 vs R as obtained from simulations

Chapter 6

Summary and Conclusions

We have developed a novel multi-phase field model with grand-potential formulation to study the influence of interface diffusion on coupled growth of ferrite and cementite during pearlite transformation. The key feature of our model is that it incorporates the real thermodynamic data from CALPHAD database, which is a new approach in this domain. In our model we approximate the free energy data using parabolic equation which are functions of temperature and composition. Some of the parameters have been expressed in terms of chemical potential instead of composition as the independent variable, which is the fundamental technique in grand potential formulation. The slope and curvature of the parabola contain important information about the properties of a particular phase. The strategies described in our model can be generally applied to study phase transitions in a variety of materials. Using our model, we have successfully simulated pearlite growth by implementing interface diffusion, which provides significant insights on the long-existing gap between the experimental and theoretical measurements reported in literature in the past.

We also perform analytical calculations using the classical Jackson-Hunt theory to support our results obtained from the model. We modify the governing equations to include interface

diffusivity in the calculations, which ultimately gives a relation between the growth velocity and inter-lamellar spacing at a fixed under-cooling. This relationship includes the ratio of interface to bulk mobility denoted by 'R' which drives the behavior of the velocity and spacing relation. Similar behavior is also achieved from phase-filed simulations. The major findings of our analysis are as follows

1. Phase-field simulations for pearlite growth suggests that addition of interface diffusion increases the growth velocity of pearlite. Interface diffusion increases the overall rate of diffusion by providing extra path for carbon atoms to diffuse through during coupled growth and hence increases the growth velocity. However it does not play a role in the selection of the inter-lamellar spacing.

2. We have studied the effect of asymmetric mobilities of $\alpha - \gamma$ and $\theta - \gamma$ interfaces on pearlite growth kinetics, keeping the volume-fraction average mobility of the growth front constant. Phase-field simulations suggest that having asymmetric mobilities of ferrite and cementite interfaces reduces the growth velocity as compared to having equal mobilities for the interfaces. However, the reduction in velocity also depends on the type of asymmetry i.e. when $\theta - \gamma$ interface has higher mobility than $\alpha - \gamma$ interface and vice versa. It is observed that $\alpha - \gamma$ interface is more dominant in controlling the growth rate, which could be due to its higher volume fraction.

3. We obtain the dependence of maximally growing velocity on ratio of interface to bulk mobilities. From our simulations it is observed that square of velocity is proportional to R, the ratio of interface to bulk mobilities. This supports our analytical calculation which also predicts the same

Chapter 7

Future Work

Appendix A

Numerical Methods

A.1 methods

Bibliography

[1] D. Brown and N. Ridley. Rates of nucleation and growth and interlamellar spacings of pearlite in a low-alloy eutectoid steel. *J. Iron Steel Inst*, 204(811-816):31, 47, 63, 66, 67, 68, 1966. 8

[2] J. W. Cahn and W. C. Hagel. Theory of pearlite reaction in v. f. zackay and h. i. aaronson, editors, decomposition of austenite by diffusional processes. *New York, Intersciences*, 12: 26, 29, 31, 66, 72, 1962. 7

[3] A. Choudhury and B. Nestler. *Phys.Rev.E*, 85(021602), 2011. iv, 20, 25, 27, 28, 30, 33

[4] K. Hashiguchi and J. S. Kirkaldy. Pearlite growth by combined volume and phase boundary diffusion. *Scandinavian Journal of Metallurgy*, 13(240-248):31, 51, 52, 57, 63, 65, 66, 1984. 8

[5] M. Hillert. The role of interfacial energy during solid state phase transformations. *Jernkont Ann*, 141(757-89):3, 23, 28, 94, 117, 1957. iii, 1, 4, 7

[6] M. Hillert. On theories of growth during discontinuous precipitation. *Metallurgical Transactions*, 3(2729-2741):3, 23, 24, 27, 47, 48, 1972. iii, 6

[7] J. D. Hunt K. A. Jackson. Lamellar and rod eutectic growth. *T Metall Soc AIME*, 226 (1129), 1966. 11, 13

[8] M. Apel K. Nakajima and I. Steinbach. The role of carbon diffusion in ferrite on the kinetics of cooperative growth of pearlite: A multi-phase field study. *Acta Materialia*, 54 (3665-3672):30, 71, 72, 73, 79, 2006. iii, 2

[9] A. S. Pandit and H. K. D. H. Bhadeshia. Mixed diffusion-controlled growth of pearlite in binary steel. *Proceedings of Royal Society A*, 467(508-521):33, 54, 71, 82, 94, 95, 99, 114, 2011. 2

[10] Plapp M Steinbach I. *Continuum Mech Therm*, (9-11), 2011. 2

[11] B. E. Sundquist. The edgewise growth of pearlite. *Acta Metallurgica*, 16(1413-1427):3, 26, 45, 46, 47, 66, 1968. iii, 6, 17, 37

[12] C. Zener. Kinetics of decomposition of austenite. *Trans. AIME*, 167(550-595):3, 25, 47, 52, 56, 59, 1946. iii, 1, 4